Journal of Electronic Materials, Vol. 7, No. 1, 1978

FORMATION AND CHARACTERIZATION OF (CdZn)S FILMS AND (CdZn)S/Cu_2S HETEROJUNCTIONS

by

L. C. Burton*, B. Baron, T. L. Hench, J. D. Meakin

Institute of Energy Conversion
University of Delaware
Newark, Delaware 19711

(Received July 11, 1977)

The present status of (CdZn)S/Cu_2S thin film solar cells is reviewed. A new source design has been used to improve the (CdZn)S films. Light reflection loss has been reduced to $\sim$ 5% by texturing the (CdZn)S surface prior to Cu_2S formation. Using 90% transparent grids, current densities over 16 ma/cm^2 and open circuit voltages over 0.7 volts have been obtained, with a best power conversion efficiency of 6.29%.

key words: solar cells, photovoltaics, thin film solar cells, heterojunctions, solar energy

INTRODUCTION

An energy band diagram for the (CdZn)S/Cu_2S heterojunction is shown in Figure 1. The major anticipated advantage for this junction in comparison to CdS/Cu_2S is a reduction in the height of the conduction band step at the interface as a consequence of improved electron affinity matching. The open circuit voltage is expected to increase by the amount that the electron affinity mismatch decreases.

* Now at Department of Electrical Engineering, Virginia Polytechnic Institute and State University, Blacksburg, VA 24061

0361-5235/78/0100-0159$05.00/1

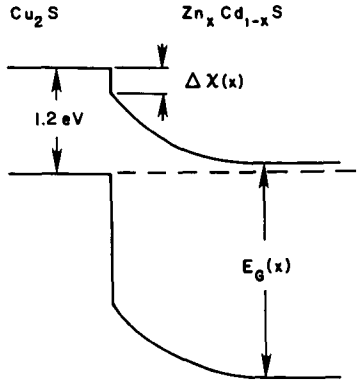

$$E_G(x) = (2.42 + 0.49x + 0.43x^2)eV$$

$$E_G(x) = E_G(0) + \Delta E_G$$

$$\Delta X(x) \sim (0.2 - \Delta E_G)eV$$

Fig. 1. Energy band diagram for the Cu_2S/(CdZn)S heterojunction.

A substantial number of reports exist in the literature on the formation and characterization of (CdZn)S crystals (1-4) and films (5-7). This material has also been studied for photovoltaic applications at the University of Delaware (8-10) and elsewhere (11,12). V_{oc} values up to 0.58 v have been reported by other investigators (11) and over 0.7 v has been measured at Delaware (8). We have verified that the increase in V_{oc} is accompanied by the expected increase in barrier height for the reverse current (9,10). The dependence of V_{oc} on zinc content is indicated in Figure 2, with the Cu_2S being formed using techniques previously described (9,10). For cells made to date, the short circuit current densities are less than for CdS cells fabricated under similar conditions.

This paper addresses improvements in (CdZn)S film formation, a reduction in light reflection and grid shading losses, and the present status of (CdZn)S/Cu_2S cells.

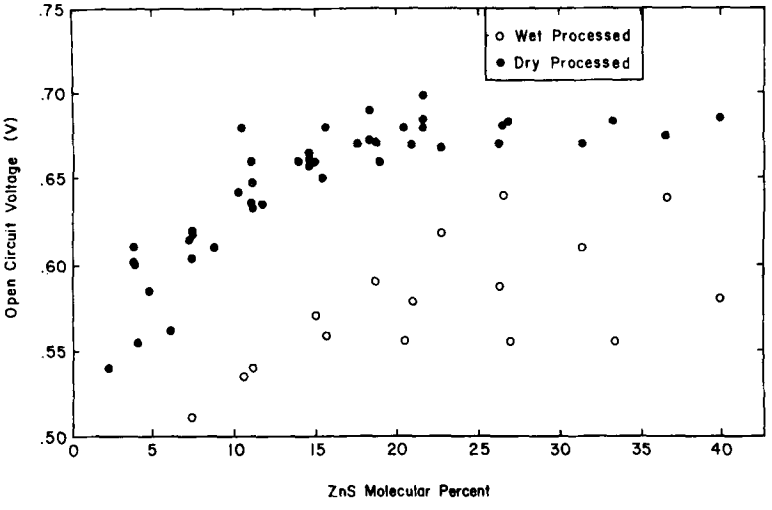

Fig. 2. Dependence of open circuit voltage on zinc content.

Film Deposition

A summary of the evolution of (CdZn)S film deposition techniques used at Delaware is given in Table 1.

The first films made by evaporating powdered (CdZn)S resulted in substantial composition gradients normal to the substrate due to preferential disassociation and evaporation of cadmium and sulfur. Evaporating from independently controlled CdS and ZnS sources gave usable films, but cells were restricted to less than 1 cm in width because of the large lateral composition gradient. More uniform composition was achieved using three identical in-line sources each machined from graphite and contained in a cylindrical tantalum heater. However, to achieve composition control the evaporation rates had to be low, necessitating low source temperatures (< 1100°C). The film resistivity has been shown to increase at low

Table 1

Evolution of (CdZn)S Deposition Techniques

Time Period	2/76-3/76	3/76-8/76	8/76-3/77	3/77-Present
Source Configuration	single source (mixed powder)	2 source	3 source	concentric source
Major Advantages	ease of operation	vertical uniformity	good overall uniformity	control of rate
Major Disadvantages	vertical composition gradient	lateral composition gradient	poor control and reproducibility	small vertical gradient

temperatures, and as a consequence the three source method places a lower bound on the reproducibly achievable resistivity. To avoid this problem, a new type of source has since been designed and initial depositions made. A cross-section of this source is shown in Figure 3. The source is machined from graphite and is surrounded by a cylindrical tantalum resistance heater. The filter is quartz wool, contained in a small cylindrical graphite chamber. This concentric design has the following advantages: 1) the single resistanceheater gives better control and reproducibility, 2) relative evaporation rates are determined by the physical parameters of the source (13) and 3) higher source temperatures can be more easily controlled, yielding lower resistivity films.

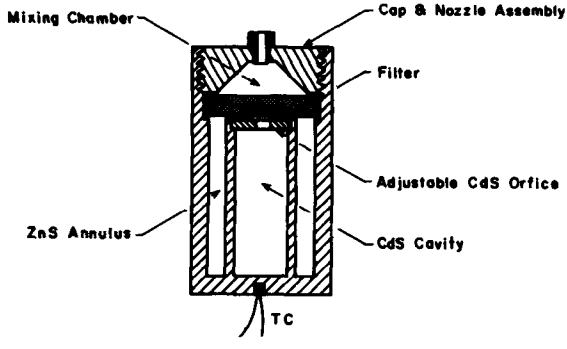

Fig. 3. Cross-section of concentric graphite source currently used for (CdZn)S deposition.

Films in the 0-60% zinc range have been made using this source. Mappings of the lattice parameter by means of x-ray analysis (8) indicate that the lateral uniformity in zinc composition is ±5%. A resistivity of 1 Ω cm has been obtained for a 10% zinc film in comparison to a resistivity of 50-100 Ω cm produced using the multi-source technique. The films produced to date show that 15-20% zinc films with resistivities of 1-10 Ω cm are achievable.

Photovoltaic Junctions

Higher open circuit voltages for the mixed sulfide cells have in general been accompanied by reduced short circuit current (9). The reduced current can result from four major causes: 1) a spike in the conduction band at the interface, 2) reduced absorption coefficient and electron diffusion length in the copper sulfide (14), 3) reflection and grid shading losses at the cell surface and 4) inadequate electric field and mobility in the mixed sulfide depletion region (15).

Referring to Figure 1, the (CdZn)S band gap dependence on composition parameter X was found to be

$$E_G(x) = (2.42 + .49x + .43x^2)\ eV$$

Assuming that the location of the $Zn_xCd_{1-x}S$ valence band edge is fixed (16), the electron affinity mismatch will decrease by about the same amount that the band gap increases i.e.

$$\Delta\chi\ (x) \tilde{-} (0.2 - \Delta E_G)\ eV$$

with an electron affinity mismatch of 0.2 eV between CdS and Cu_2S being assumed (17).

These relations, and open circuit voltage and barrier height measurements, indicate that a conduction band spike should occur in the 25-30% zinc range. For higher zinc content, the current density decrease is caused primarily by the conduction band spike at the interface. (The levelling off of V_{oc} in Figure 2 at ~25% zinc is caused in part by the sharp decrease in short circuit current that occurs). Since our Cu_2S has good stoichiometry ($x \geq 1.996$ in Cu_xS) with resistivity > 0.1 Ω cm, mechanism two, above, is probably not significant. The lower currents for zinc content less than ~25% are thus apparently due to mechanisms not associated with the band spike or bulk properties of the Cu_2S.

The principle remaining mechanisms are related to the reflection and shading losses, and to the electrical properties of the mixed sulfide. For cross comparisons between (CdZn)S and CdS current densities, the optical effects can be made constant by using the same type of grid and surface texturing on both materials. However, it must be verified that the (CdZn)S surface can be textured in a manner similar to CdS, thus reducing reflection loss, before the other loss due to mechanisms in the mixed

sulfide can be identified. With respect to the anti-reflection effects produced by an HCl etch (55% HCl by volume at 60°C), we have shown that the two materials behave in a similar manner. This is indicated in Figure 4 and Table 2. The effect of the etch on the surface topography is seen in the micrographs and is verified by the total reflectivity values given in the table. After the formation of the Cu_2S on the etched surface, the reflectivity is about 5% (4 sec etch - no grid or AR coating present).

Table 2

Total Reflectance Data for CdS and (CdZn)S Surfaces

Sample	% Zn	Before Etch(5)	Etch Time(sec)	After Etch(%)	After Barrier(%)
465	0	25	4	15	5
424	12	21	4	10	5
490-2	21	22	2	12	7
490-4	21	22	4	12	5

The substantial effects of post-gridding heat treatments for mixed sulfide cells are evident in Figs. 5 and 6. In Figure 5 it is seen that I-V parameters (V_{oc}, J_{sc}, fill factor and efficiency) and stability are dependent on heat treatment history, as is the case for the CdS cell. One result of heat treatment that appears different for the two materials relates to the diffusion of copper from the Cu_2S into the n-region. The strong dependence of CdS/Cu_2S junction behavior (both light and dark) on the compensated region in the CdS has been established (15,18).

Junction capacitance values for mixed sulfide cells do not decrease as rapidly with heat treatments as do those for CdS/Cu_2S cells, indicating that copper diffuses more slowly into the mixed sulfide from the Cu_2S. The dependence of light generated current on the compensated (copper diffused) region is expressed by the relation (15)

$$j_L = j_{LO} \frac{\mu F}{\mu F + S}$$

where j_L = light generated current collected
j_{LO} = light generated current with no interface recombination
μ = electron mobility in n-region depletion layer

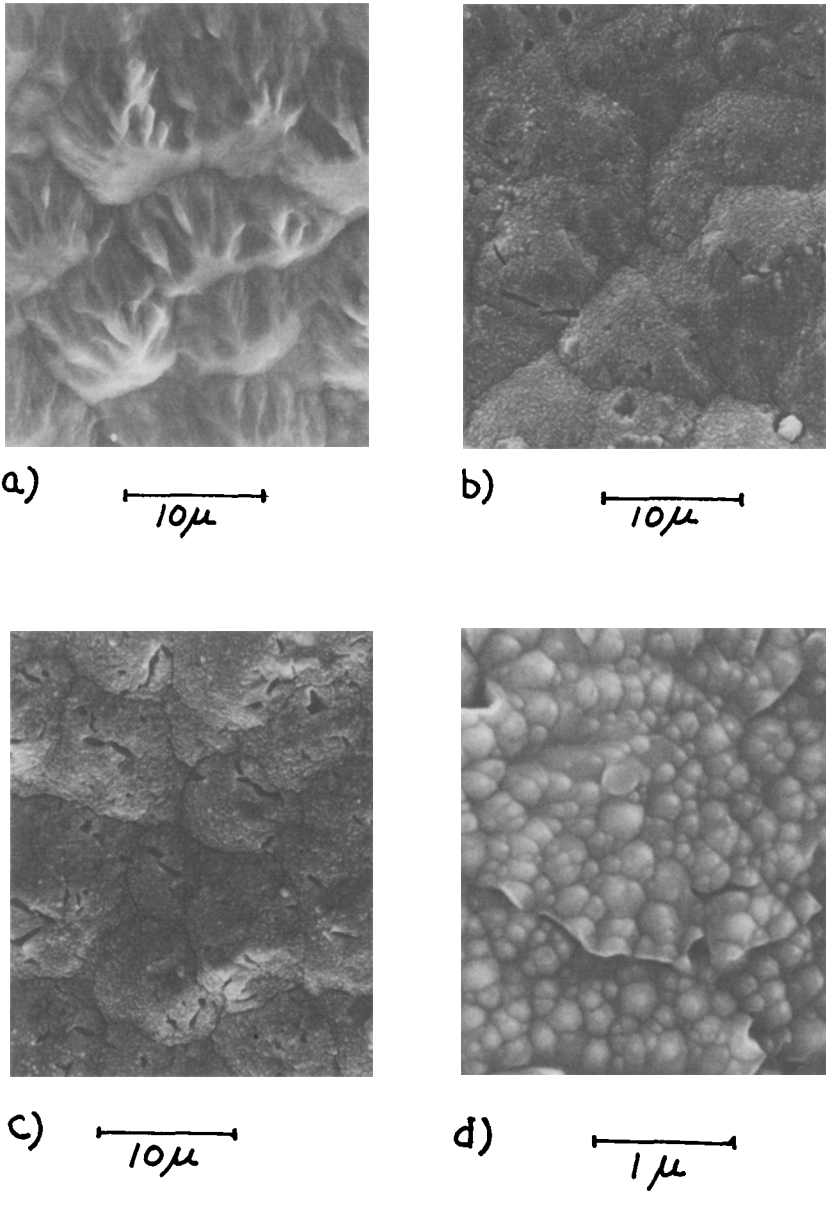

Fig. 4. Scanning electron micrographs of textured (CdZn)S surfaces. Etch times were none (a), 2 sec (b), and 4 sec (c) and (d)

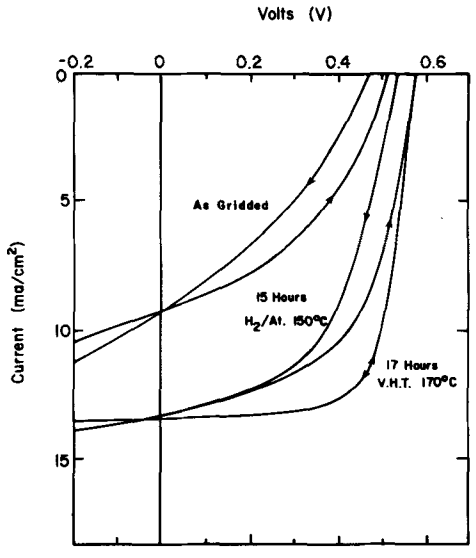

Fig. 5. Effect of heat treatments in 10% hydrogen-90% argon and vacuum (V.H.T.) on response and stability of mixed sulfide cell.

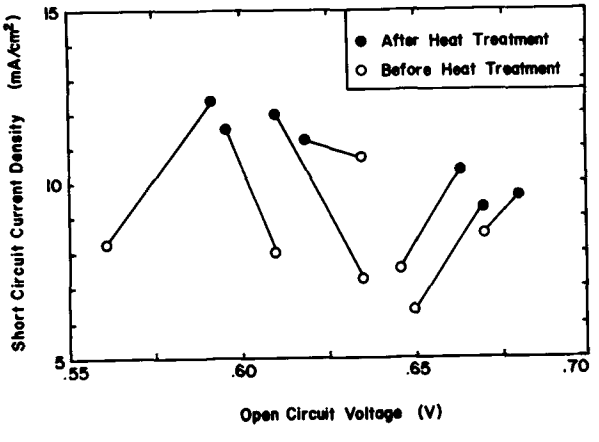

Fig. 6. J_{SC} and V_{OC} changes for several mixed sulfide cells as a consequence of heat treatment in 10% hydrogen-90% argon ambient.

F = electric field at edge of depletion layer
S = interface recombination velocity

j_{LO} is generated almost entirely in the Cu_2S and the question is whether the other terms are significantly different for the mixed sulfide. The electric field is determined by the junction charge profile, which is controlled by the bulk resistivity as modified by copper compensation. Reduced electron mobility could be expected in the mixed sulfide, but the effect on current density is dependent on the relative magnitudes of μF and S. The improved lattice match at the (CdZn)S/Cu_2S interface should reduce the interface state density and hence S, but the electron capture cross section may also be varying. Even for the more extensively studied CdS/Cu_2S junction, these parameters have not been determined to the precision necessary to predict J_{SC} to better than ± 10%, thus the role they play for the mixed sulfide junction remains obscure. The quantitative analysis of current loss mechanisms in the mixed sulfide cell has not yet reached that of the CdS cell, but a major effort is currently underway at Delaware to develope this analysis.

Current-voltage characteristics under actual sunlight for two of the best mixed sulfide cells are given in Figure 7, for V_{OC} values of 0.64 and 0.68 volts. The grids on these cells are only about 90% transparent, and no AR coatings were used. Previous experience shows that application of our best gridding and AR technology to these cells will result in more than 10% improvement in efficiency.

The currents and voltages achieved to date show that the present cell design is capable of power conversion efficiencies over 7.5%. The application of advanced gridding and AR technology developed for the CdS/Cu_2S cell, along with further optimization of the mixed sulfide, should results in further improvements in cell efficiency.

Acknowledgements

This work was supported by NSF-RANN Grant AER 72-03478 and ERDA Grant E(49-18)-2538. We also appreciate the reviewers excellent comments.

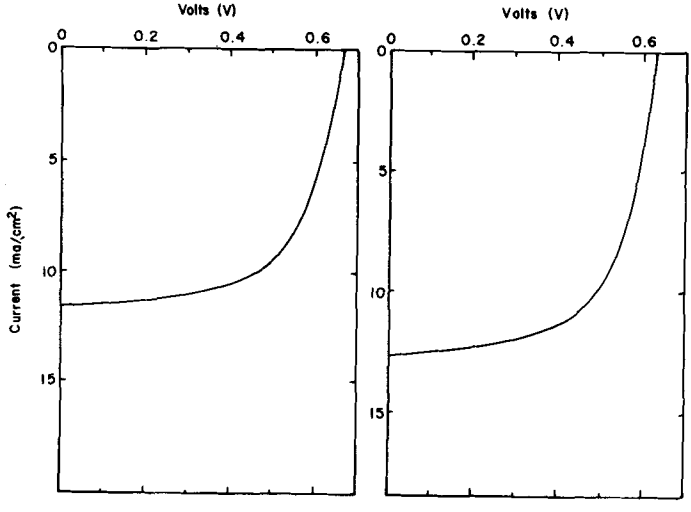

CELL 418B1		CELL 413E2
83.7	INSOLATION (MW/CM^2)	80.9
0.68	V_{OC} (v)	0.64
11.9	J_{SC} (MA/CM^2)	12.7
61.3	FF %	62.3
5.87	EFFICIENCY %	6.29
14.2	J_{SC} (100 MW)	15.7

Fig. 7. Current-voltage characteristics for two of the best mixed sulfide cells. Grids are ∿ 90% transparent and cells have no AR coatings.

References

1. D. W. G. Ballantyne and B. Ray, Physica 27, 337 (1961).

2. R. B. Lauer and F. Williams, J. Appl. Phys. 42, 2904 (1971).

3. M. J. Kozielski, J. Crystal Growth 30, 86 (1975).

4. L. G. Suslina, E. I. Panasyuk, S. G. Konnikov and D. L. Fedorov, Sov. Phys. Semicond. 10, 1093 (1976).

5. W. Kane, J. Spratt, L. Hershinger and I. Khan, J. Electrochem. Soc. 113, 136 (1966).

6. D. Bonnet, Phys. Stat. Sol. (a) 11, K135 (1972).

7. D. B. Fraser and H. D. Cook, J. Vac. Sci. Technol. 11, 56 (1974).

8. L. C. Burton and T. L. Hench, Appl. Phys. Lett. 29, 612 (1976).

9. L. C. Burton, B. Baron, W. Devaney, T. L. Hench, S. Lorenz and J. D. Meakin, Proceedings of the 12th IEEE Photovoltaic Specialists Conference, Baton Rouge, LA. (IEEE, New York, 1976), p. 526.

10. Progress Reports NSF/RANN/AER72-03478 A04 FR76, E(49-18)-2538 PR76/1, E(49-18)-2538 PR 76/2, Institute of Energy Conversion, University of Delaware (1977).

11. W. Palz, J. Besson, T. Nguyen Duy, and J. Vedel, Proceedings of the 10th IEEE Photovoltaic Specialists Conference, Palo Alto, CA (IEEE, New York, 1973).

12. T. M. Peterson, Ph. D. Thesis (Lawrence Berkely Laboratory, University of California at Berkely, 1975).

13. D. Beecham, Rev. Sci. Instrum. 41, 1654 (1970).

14. L. C. Burton and H. M. Windawi, J. Appl. Phys. 47, 4621 (1976).

15. A. Rothwarf, Technical Report NSF/RANN/AER 72-03478 A04/TR76/1, Institute of Energy Conversion, University of Delaware (1976).

16. J. O. McCaldin, T. C. McGill and C. A. Mead, J. Vac. Sci. Technol. 13, 802 (1976).

17. A. Rothwarf and A. M. Barnett, IEEE Transactions on Electron Devices ED-24, 381 (1977).

18. L. R. Shiozawa, F. Augustine, G. A. Sullivan, J. M. Smith III and W. R. Cook, Jr., Clevite Final Report No. AR1 69-0155 (Clevite Corporation, Cleveland, 1969).